
Omni-Video: Democratizing Unified Video Understanding and Generation

Zhiyu Tan^{1,2†} Hao Yang^{2†} Luozheng Qin² Jia Gong² Mengping Yang^{2*} Hao Li^{1,2*}

¹Fudan University ²Shanghai Academy of Artificial Intelligence for Science

Project Page: https://howellyoung-s.github.io/OmniVideo_project/

Abstract

Notable breakthroughs in unified understanding and generation modeling have led to remarkable advancements in image understanding, reasoning, production and editing, yet current foundational models predominantly focus on processing images, creating a gap in the development of unified models for video understanding and generation. This report presents *Omni-Video*, an efficient and effective unified framework for video understanding, generation, as well as instruction-based editing. Our key insight is to teach existing multimodal large language models (MLLMs) to produce continuous visual clues that are used as the input of diffusion decoders, which produce high-quality videos conditioned on these visual clues. To fully unlock the potential of our system for unified video modeling, we integrate several technical improvements: 1) a lightweight architectural design that respectively attaches a vision head on the top of MLLMs and a adapter before the input of diffusion decoders, the former produce visual tokens for the latter, which adapts these visual tokens to the conditional space of diffusion decoders; and 2) an efficient multi-stage training scheme that facilitates a fast connection between MLLMs and diffusion decoders with limited data and computational resources. We empirically demonstrate that our model exhibits satisfactory generalization abilities across video generation, editing and understanding tasks. Our code will be publicly available at: <https://github.com/SAIS-FUXI/Omni-Video>.

1 Introduction

The remarkable advancement of artificial intelligence in recent years, especially multimodal understanding [1, 2] empowered by large-language models (LLMs) and multimodal generation[3, 4, 5] models driven by diffusion models, has enabled thrilling possibilities to go beyond existing experiences across various modalities, including vision [6, 7, 8, 9], language [10, 11, 12], as well as audio [13, 14, 15, 16], etc. Despite these progresses, most understanding and generation systems are often designed separately, *i.e.*, each specialized for a specific task or modality, leading to significant modeling redundancy and laborious computing complexity. Alternatively, unified multimodal models [17, 18] have emerged as a promising solution and gained increasing attention for their ability to input/output diverse data types seamlessly. Such unified pipeline is trained jointly across multiple modalities to model task-agnostic representations [19, 20] within a single framework, thereby removing tailored modality-specific components while achieving strong performance on both individual and compositional tasks [21, 22].

Following this philosophy, recent efforts [23, 24] have focused on developing unified architectures that simultaneously handle multimodal understanding and generation tasks. Considering that the

† Equal Contribution.

* Corresponding Authors.

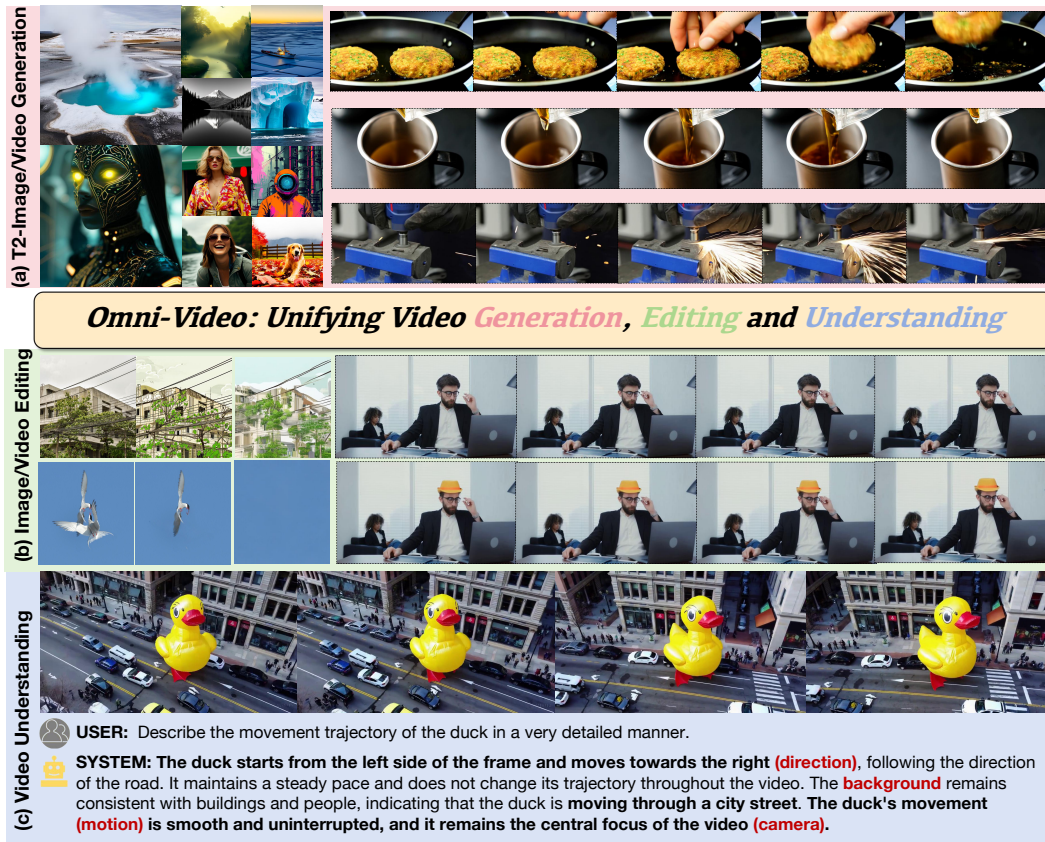


Figure 1: **Comprehensive illustration of the fundamental capabilities of our *Omni-Video*** on (a) photorealistic text-to-image/video generation, (b) image/video editing (*i.e.*, change the style of source image toward target image and remove objects in the source image), and (c) video understanding (describe directions, background, motion, and camera movement, *etc.*), all these tasks could be accomplished within a single unified architecture.

transformer-based autoregressive (AR) architecture serves as the predominant architectural paradigm for multimodal understanding, earlier approaches project both texts and images into discrete tokens to facilitate AR modeling across modalities [17, 25]. For instance, Emu3 [25] tokenize images, texts, and videos into a discrete space and train a single transformer model via next-token prediction on these multimodal sequences. Chameleon [26] designed an early fusion scheme to project all modalities into a shared discrete representational space for better interaction and reasoning. Motivated by the great success of diffusion models [4, 3] in visual generation, the most recent works [23, 24] design hybrid diffusion-AR architectures that incorporate diffusion decoders to translate high-level visual tokens into photorealistic outputs. Representative works such as Transfusion [27] and Show-O [28] respectively employ continuous and discrete diffusion modeling with full attention for improved visual quality.

However, training the above unified models from scratch requires substantial computational resources and a massive amount of multimodal data. Additionally, integrating MLLMs and diffusion models within a unified system poses significant challenges in architectural modifications and hyperparameter tuning. To tackle these challenges, MetaMorph [18] demonstrated that an improved visual understanding inherently endows MLLMs with visual generation capabilities. Building on this insight, a straightforward visual predictive instruction tuning (VPiT) strategy was introduced to train LLMs to generate continuous visual tokens, which are subsequently decoded into plausible images using a modified diffusion model. Accordingly, MetaMorph achieved competitive performance on both image understanding and generation tasks with minimal architectural changes and computational overhead. Nevertheless, previous unified models have predominantly targeted static images and show

limited capability when it comes to processing videos, where accurately modeling temporal dynamics, ensuring motion coherence, and maintaining frame-wise consistency are essential. Furthermore, the elevated data and computational demands for video modeling impose significant scalability constraints on current unified frameworks. Consequently, delivering an appropriate framework for unified video understanding and generation is critically important for immersive media understanding, production, and even interaction.

To fill the vacant, this technical report proposes *Omni-Video*, an efficient and effective framework for unified video understanding and generation that combines a lightweight architectural design with a multi-stage training scheme. Borrowing the exceptional video understanding and generation capabilities of existing MLLMs (e.g., VILA [29]) and text-to-video (T2V) diffusion (e.g., Wan [5]) models, our method aims at teaching existing video understanding MLLMs to produce video tokens that are ‘understandable’ for existing T2V diffusion models. More specifically, we first tuning MLLMs to produce textual tokens and visual tokens with separate text and vision heads following [18], the vision head generates continuous video tokens that is aligned with the representation of a pretrained vision encoder, e.g., SigLIP2 [30]. Then, we adapt the continuous video tokens into the T2V diffusion model’s conditional space with a dedicated lightweight adapter, such that the T2V model could synthesize faithful videos directly from the continuous video tokens. Notably, only a small subset of model parameters, i.e., the text and vision head in stage-1 and the adapter in stage-2, are optimized. To further activate the potential visual generation capability of MLLMs, we unlock the parameters of text and vision head, adapter, as well as the T2V model and train the whole system with meticulously curated high-quality understanding and generation data, thereby improving the synthesis quality and the understanding ability. This selective fine-tuning strategy requires only minimal data and computational resources, allowing for efficient adaptation without compromising the foundational performance of the pretrained model.

In addition to generate harmonious videos conditioned on user instructions, we also extend our unified framework towards detail-preserving visual editing scenarios. One straightforward solution is to feed original signals into the visual encoder of MLLMs and retrain the unified model to reconstruct unedited areas and penalize editing areas with paired editing data[31, 32, 33]. This approach, however, incurs substantial computational overhead with massive data and often leads to suboptimal performance as MLLMs primary focus on high-level semantic features rather low-level details. Since T2V diffusion models are trained to recover clean videos from corrupted signals, they inherently excel at processing fine-grained visual information. Accordingly, we leverage pretrained VAEs to extract low-level compressed priors from original input and directly send them to the diffusion model. Such that, the original signals interact with noised embeddings throughout all denoising steps, ensuring high-fidelity visual preservation during the editing process. Furthermore, motivated by the recent chain-of-thought reasoning capabilities in the LLMs community, we devise a “think mode” to achieve higher-quality visual outputs through logical inference and contextual planning in video generation and editing. Together, our framework enables seamlessly predicting multimodal tokens for video understanding, generation, as well as video editing tasks, with minimal architectural modification, diverse data sources, and computation-efficient optimization.

In order to testify the effectiveness of our proposed *Omni-Video*, we conduct extensive experiments across various tasks including image/video understanding, text-to-image/video generation, image/video editing (Fig. 1). The results demonstrate that our method achieves favorable results on these tasks within a unified model. Notably, the integration of a chain-of-thought reasoning module (“think mode”) yields better understanding of users’ instructions and obtains consistent improvements in output quality, suggesting the great potential of inference time scaling in unified models. To sum up, our primary contributions are summarized below:

- **A unified paradigm for video unified modeling:** We introduce *Omni-Video*, a novel framework that integrates video understanding and generation. By teaching the multimodal understanding model to produce continuous vision tokens for diffusion to generate realistic videos, our model successfully tackles complex video understanding and generation within a single model.
- **An efficient multi-stage training receipt for resource-friendly optimization:** We devise a mutl-stage training scheme that accomplish 1) fast alignment between MLLMs’ visual tokens and pre-trained visual encoder, and 2) efficient adaptation of the visual token toward T2V models’ conditional space. Accordingly, our model is effectively trained without massive computation resources.

- **A thorough empirical evaluation demonstrates superior performance:** Extensive experiments under various video understanding and generation scenarios demonstrate that *Omni-Video* achieves prevailing performance. Moreover, the integration of video/image editing enhances the model’s flexibility as a general-purpose framework.

2 Related Work

2.1 Multimodal Understanding

Taking advantage of advanced large language models (LLMs) [34, 35, 36], multimodal large language models (MLLMs) have gained extensive research attention and demonstrated magnificent capabilities in understanding and reasoning multimodal content [37, 2, 38]. In order to inject knowledge beyond the text modality into LLMs, existing methods typically employ modality-specific encoders (*e.g.*, CLIP [39]) to extract latent embeddings and perform alignment within the LLMs’ transformer space. For instance, LLAVA [40, 41] and MiniGPT-4 [42] connect pre-trained visual encoders and LLMs with simple projection layers, enabling LLMs to perform complex multimodal understanding while preserving their textual reasoning ability. Building this insights, more advanced techniques such as scaling the visual encoders [1], support dynamic and high input resolutions [43], employment of Mixture-of-Experts (MOE) architectures [44, 45], replacing linear projection layers with different architectures [46, 47], improvement of training receipts [48, 29] are developed to enhance the fine-grained perception capabilities of MLLMs. Similarly, video-centric MLLMs [29] encode videos into sequential visual tokens that are compatible with LLMs. Although these approaches excel at multimodal understanding and reasoning, they primarily focus on perception tasks and lack the capability of producing other modalities beyond text.

2.2 Multimodal Generation

Early multimodal generation models employ generative adversarial networks (GANs) [49] to synthesis novel outputs. However, the scalability, visual quality and resolution of GANs are relatively poor. Diffusion models (DMs) [50] and autoregressive (AR) models [51, 52], equipped with their inherent stable optimization and scalability, the transformer architecture, large-scale training and infrastructure, and trillion-level multimodal corpus, are current state-of-the-art for image/video synthesis.

Diffusion models (DMs). DMs gradually transform simple noise distributions into complex data distributions through a series of learned denoising steps. The pioneering work laid the theoretical foundations, while numerous subsequent studies have enhanced the efficiency and output quality through improved training/sampling strategies [53, 54, 4, 55] and optimization techniques [56, 57, 58], *etc.* In particular, the introduction of stable diffusion (SD) and diffusion transformer (DiT) [59] directly caused the blooming of high-quality, high-resolution, and long-duration visual generation. For instance, Sora [60], built on the diffusion transformer architecture, achieved superior performance in producing detailed, high-resolution videos that adhere to the user’s instructions. Follow-up approaches including open-sourced [61, 62, 5] and closed-source models [63, 64] have further advanced the state-of-the-art in text-to-video generation. These developments underscore that enhanced diffusion techniques are enabling richer, more dynamic, and semantically coherent visual content creation. In this work, we integrate the open-sourced Wan2.1 [5] video generation model into our unified understanding and generation system as its leading performance in the open-source community.

Autoregressive (AR) models. Borrowing the success of AR modeling in language domain, another line of approaches learn to synthesize visual content in autoregressive manner. Concretely, visual inputs are first mapped into a sequence of discrete tokens, after which both visual and text tokens are modeled via next token prediction. To encode continuous visual signals into discrete tokens, vector quantization techniques [65, 66, 67] are usually applied to high-dimensional data into a finite set of latent codes (codebook). DALLE [68, 3] demonstrated that scaling with sufficient data autoregressively could generate high-quality images from textual descriptions. MAGVIT-v2 [65] showed that GPT-style LLMs might outperform diffusion models on visual generation benchmarks with an improved video tokenizer. With this top-performing tokenizer, VideoPoet further identified the potential of AR model, which was trained on discrete visual, text and audio latents, in producing plausible videos, especially excel in modeling complex large motions. Differently, VAR [66] designed a coarse-to-fine “next-scale prediction” paradigm to learn visual distributions and MAR [67] applied AR modeling in the continuous space by modeling per-token distribution by diffusion.

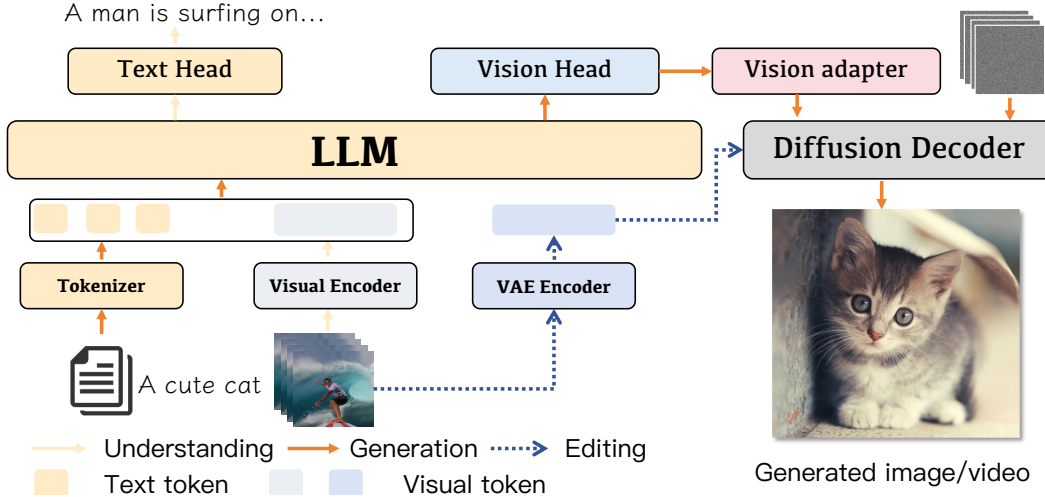


Figure 2: **Overall architecture of our proposed *Omni-Video* for unified video understanding and generation.** We connect MLLMs’ exceptional understanding capability with the visual generation ability of diffusion decoders with lightweight architectural design, enabling MLLMs to produce visual continuous tokens that are decoded into photorealistic images/videos by the diffusion decoder.

2.3 Unified Multimodal Understanding and Generation

In an effort to build a single system for both understanding and generation tasks, substantial developments have been witnessed in unified multimodal models recently. In addition to the text modality, these models process various modalities as input (*e.g.*, image, video) and also output various modalities in a unified manner. Depending on whether visual signals are encoded into discrete or continuous tokens, existing unified multimodal models primarily consist of pure AR models [17, 25, 69] and diffusion-AR hybrids [18, 23, 70]. For example, both Chameleon [26] and Emu3 [25] represented image/videos with VQ-VAE [71] as discrete tokens and trained uniform transformer-based LLM models from scratch in next token prediction manner. Janus and Janus-pro [17] decoupled visual encoding with SigLIP [72] and VQ-VAE [73] for multimodal understanding and generation, respectively. Such decoupling ameliorated the conflict of visual encoder for understanding and generation tasks. Following this philosophy, the most recent work converted images into discrete tokens with a text-aligned tokenizer that was aligned with LLM embeddings. However, discretizing visual signals often struggles to preserve fine-grained details, leading to sub-optimal synthesis performance. Consequently, UniFluid [74] build a unified framework from continuous visual tokens following the MAR’s per-token distribution modeling.

Alternatively, other approaches integrate diffusion models into LLMs for visual decoding. In particular, Show-O [28] and Tranfusion [27] unified diffusion models for generation tasks and LLMs for textual responses, while the former adopted discrete diffusion and the latter used continuous diffusion. Along this line, Show-O2 [75] and Mogao [70] improved the model performance via combining AR modeling and flow-matching [76]. In order to identify the impact of core components (*i.e.*, image representation, training objective, training strategies) of hybrid diffusion-AR unified models, BLIP3-o [23] presented a thorough empirical study. Despite these models’ success in unifying understanding and generation, training these models from scratch requires massive compute and data resources. The most related work to ours is MetaMorph, which trained LLMs to predict multimodal tokens for generation with visual-predictive instruction tuning (VPiT). However, most of existing methods, including MetaMorph, focus on modeling static images and show very limited ability for processing videos. Therefore, this work presents an efficient and effective framework for unified video understanding and generation.

3 Model Architecture

3.1 Overview

Recall that our aim is to build a unified architecture that enables multimodal video understanding and generation simultaneously. To achieve this, we teach multimodal understanding models (e.g., VILA [29]) to produce visual tokens as the input of a text-to-video diffusion model with lightweight adapters and a novel three-stage training scheme. In this way, the alignment between the output visual tokens and the diffusion model’s context conditions could be achieved efficiently, without requiring training the whole system from scratch. Fig. 2 presents the overall structure of our *Omni-Video*. Overall, our model connects an AR-based MLLM model for understanding and a DiT-based diffusion model for visual generation, more details are presented below.

3.2 Producing Visual Tokens with MLLMs

Prior MLLMs accept both textual tokens and visual embeddings but only produce textual tokens, to support both textual and visual outputs within a unified MLLM model, we design two distinct prediction heads, *i.e.*, one **Text Head** for textual output and one **Vision Head** for visual output. Formally, given a multimodal input consisting of M textual tokens $T = \{t_1, t_2, \dots, t_M\}$, with each token $t_j \in T$ drawn from a fixed vocabulary \mathcal{T} , and N visual content represented as embeddings $V = \{\mathbf{v}_1, \mathbf{v}_2, \dots, \mathbf{v}_N\}$, where each embedding $\mathbf{v}_t \in \mathbb{R}^D$ represents embeddings of one frame extracted from pre-trained visual encoders. Our unified MLLM model seeks to jointly model this combined input sequence $I = [T; V]$ and producing $O = [T_o; V_o]$, where T_o and V_o respectively represent textual tokens from the text head and visual outputs from the vision head.

More specifically, the text token performs standard language modeling, predicting tokens from a vocabulary augmented with four newly introduced special tokens: <BOI>, <EOI>, <BOV>, and <EOV>. Conversely, the vision head maps the MLLMs’ hidden states into a continuous visual tokens. To enforce strong semantic grounding and stable latent predictions, the vision head is trained to align the continuous visual embeddings extracted by off-the-shelf visual encoders (e.g., SigLIP-v2[30]). Such alignment can be accomplished by computing the similarities (e.g., L2 distance, cosine similarity) between the visual tokens V_o from vision head and visual embeddings E from the pre-trained visual encoders:

$$\mathcal{L}_{vision} = \|V_o - E\|^2. \tag{1}$$

Regarding the text head, it aims to predict text sequences $\hat{T} = [\hat{t}_1, \hat{t}_2, \dots, \hat{t}_{m'}]$ from the input of $T = [t_1, t_2, \dots, t_m]$. This sequence is optimized according to the cross-entropy loss defined as:

$$\mathcal{L}_{text} = - \sum_{j=1}^m \log P(\hat{t}_j | t_j). \tag{2}$$

Once trained, the two distinct heads are separately responsible for generating textual outputs for understanding tasks and visual tokens for generation tasks. Such explicit modality-marking modality-marking strategy not only resolves ambiguity but also significantly enhances the coherence and fidelity of multimodal generation. Notably, only the vision head and the text head are trained, which maintains the original multimodal understanding capabilities of MLLMs to a great extent and efficiently turns understanding-only MLLMs to generate visual clues.

3.3 Making Visual Tokens Understandable for DMs

After finetuning a pre-trained MLLM to synthesize both visual and text tokens with separate heads, we turn to decoding the output visual tokens as photorealistic images and videos. Inspired by the great success of diffusion models (DMs) in the context of image and video generation, we incorporate pre-trained T2V diffusion models as our visual decoder. Along this line, we design a dedicated lightweight adapter to project the visual context sequences V_o from the vision head into a compact embedding space that is “understandable” for the diffusion model. Formally, given the output V_o tokens, the adapter process them as:

$$Q = \text{Adapter}(V_o), \tag{3}$$

where Q denotes the output of the adapter and is further adopted as the input condition of the diffusion decoder, guiding the diffusion decoder to generate images that are harmonious to the input instructions.

To make sure that the diffusion decoder could produce high-quality visual contents conditioned on Q , we devise an effective training strategy: we first explicitly align the adapter’s outputs with the conditional space (*i.e.*, the textual embedding derived from text encoders) of the diffusion decoder, thus bridging the domain gap between multimodal context representations and the diffusion decoder’s conditioning space. Then, we train the adapter with real-world paired text and visual images/videos with the diffusion decoder’s training objective:

$$\mathcal{L}_{\text{DMs}}(\theta) = E_{(X_1, Q) \sim D, t \sim U(0,1), X_0 \sim N(0,1)} [\|V_\theta(X_t, Q, t) - V_t\|^2], \quad (4)$$

where θ denote the model’s parameters, it is noteworthy that only the lightweight adapter is updated here, thus θ is the adapter’s parameters. $V_\theta(X_t, Q, t)$ denotes the predicted velocity based on an instance (X_1, Q) , timestep t , and noise X_0 , and Q is the output of the adapter. This alignment significantly enhances the semantic consistency of the generated outputs while enabling efficient and stable training.

3.4 Unifying Understanding, Generation and Editing

In addition to supporting visual generation tasks, we further integrate the challenging video editing tasks into our unified framework. Video editing requires the model to reliably understanding user instructions and precisely editing specific areas while preserving other details. To achieve this, we introduce two generation modes for video generation and editing based on their conditional inputs. In the generation mode, the adapter exclusively processes latents predicted by the vision Head along with corresponding textual embeddings, then the diffusion decode produce videos conditioned on the adapter’s output. In contrast, when operating in editing mode with source condition videos available, we enhance the input to the adapter by incorporating sequence embeddings of these source videos. These embeddings are extracted using a visual compressor, specifically a 3D-causal-VAE. In this way, we can effectively integrate the spatial and temporal features of the source videos into the editing process.

Concretely, for each sample, we concatenate the following modalities into a unified conditional embedding sequence: $\mathbf{c} = [\mathbf{v}_1, \dots, \mathbf{v}_T \parallel \mathbf{h}_1, \dots, \mathbf{h}_{T'} \parallel \mathbf{t}_1, \dots, \mathbf{t}_m]$, where \mathbf{v}_t represents the vision latent predictions from the AR Vision Head, and \mathbf{h}_t are optional spatial-temporal embeddings derived from a pretrained 3D-Causal-VAE utilized specifically in editing scenarios. Moreover, \mathbf{t}_1 denotes the original textual conditional input of the diffusion decoder. The conditional sequence \mathbf{c} is then projected via the adapter module and subsequently injected into every block of the DiT via cross-attention mechanisms. Such explicit conditioning ensures that the diffusion model accurately adheres to the intended semantic content and retains spatial-temporal consistency across frames. During the training process, the system automatically switches between these two modes in response to generative and editing data inputs. Such adaptive mechanism ensures that the model can efficiently adjust its operational mode to optimize both generation and editing performance, thereby enhancing the overall effectiveness of the model in handling diverse data types.

4 Data and Training

4.1 Data

To train our *Omni-Video*, we use a mixture of open-source multimodal data including image understanding, video understanding, text-to-image, text-to-video, instruction-based image and video editing data. Tab. 1 and Fig. 3 present the detailed data sources used in our training. In general, our dataset comprises approximately 17.2 million samples for image understanding, 1.98 million for video understanding, 15 million for image generation, 8.6 million for image editing, 1.8 million for video generation, and 0.8 million for video editing. This sufficient distribution highlights a strong emphasis on image-centric tasks while still providing sufficient resources to support key developments in video-related research. For video understanding data, we use the original data format released by the official. For the text-to image and text-to-video data, we conduct a comprehensive data curation pipeline to obtain high-quality training data. The curation pipeline including but is not limited to: quality filtering via assessing the resolution, ratio of width and height, aesthetic prediction,

Table 1: Summary of datasets used in the joint vision and language pretraining stage.

Category	Dataset	Ratio
Image Understanding	Total	37.9%
	JourneyDB-4M [77]	
	LLaVA-v1.5 [41]	
	ShareGPT4V [78]	
	Cambrain-7M [79]	
	MMC4 [80]	
Video Understanding	Total	4.36%
	LaVA-Video-178K [81]	
	VSTaR-1M [82]	
	ShareGPT4Video-40K [83]	
Text-to-image Generation	Total	33.05%
	LAION-5B [84]	
	COYO-700M [85]	
Text-to-video Generation	Total	3.97%
	HD-VILA [86]	
Text-to-image Editing	Total	18.95%
	AnyEdit [87]	
	UltraEdit [32]	
	HIVE [33]	
	PromptFix [31]	
Text-to-video Editing	Total	1.76%
	Senorita-2M [88]	

video clipping; content filtering via evaluating watermarks, optical flow-based motion prediction, text overlays, OCR detection, *etc.* Moreover, the text conditions are re-captioned based on the visual content using a multimodal large language model.

4.2 Three-Stage Training Strategy

4.3 Training

As shown in Fig. 4, we employ a multi-stage training strategy to effectively connect multimodal understanding models (MLLMs) with text-to-video diffusion models, transforming MLLMs to to unified multimodal model. To be more specific, we first attach a separate vision head on the top of MLLMs to produce visual tokens, followed by finetuning a lightweight adapter to align the visual tokens with the conditional space of the diffusion decoder. Finally, we perform joint finetuning on both understanding blocks and generation blocks for high-quality visual generation.

Model Initialization. To mitigate the substantial training costs, we initialize the components of our unified model using readily available pretrained weights. Training either a Multimodal Large Language Model (MLLM) for video understanding or a diffusion model for video generation from scratch necessitates vast computational resources and data. Therefore, the selection of appropriate pretrained models for initialization is a critical step. For the MLLM component, we adopt the weights from VILA [29]. Regarding the diffusion model component, we initialize our model with the weights of the Wan 2.1 text-to-video model [5]. This model was chosen for its compact parameter count of only 1.3B, which still provides a strong foundation for text-to-video generation. We clarify that the original Wan 2.1-1.3B model does not natively support visual editing capabilities, and we enable the diffusion decoder to perform image and video editing tasks via the proposed method mentioned earlier. Moreover, the newly introduced adapter and vision head are initialized using a standard random initialization manner.

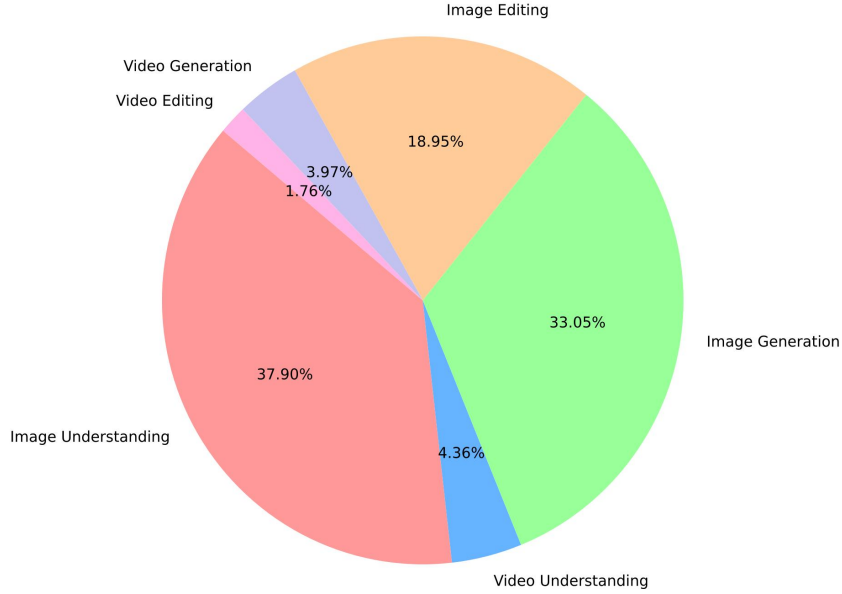


Figure 3: **Distribution of datasets used in the joint vision and language pretraining stage.**

Stage-1: Teaching MLLMs to generate visual continuous tokens. In the initial stage, we keep the parameters of the MLLM fixed, focusing solely on training the text head and vision head, with the parameters of the diffusion model also remaining unchanged. The trained loss includes: 1) the similarity loss between the visual tokens from the vision head and visual embeddings from the pre-trained visual encoders (Eq.1); and 2) the cross-entropy loss that perform next token prediction on the text sequences (Eq.2). The primary goals at this stage are twofold: Preserving the understanding capabilities of MLLMs and swiftly training the newly introduced components (*i.e.*, the vision head) to produce visual continuous tokens. During this phase, we incorporate data relevant to both understanding and generation tasks. As a result, the MLLM not only retains its video comprehension abilities but also learns to distinguish between understanding and generation tasks. When the user instructions are to generate images/videos, the vision head produce tokens between the special tokens: <BOI>, <EOI>, <BOV>, and <EOV>, which are further used as input for the diffusion decoder.

Stage-2: Projecting visual continuous tokens into diffusion models' conditional space. In the second stage, we keep all understanding-related parameters fixed and focus exclusively on training the generative modules. During this phase, we train the adapter to improve the alignment of semantic information from the understanding module with the latent space of the diffusion model. Concretely, the output visual continuous tokens from the vision head are fed to the adapter, the adapter is first trained to align its output with the textual embedding space of the diffusion decoder. Then, conditioned on the output of the adapter, we incorporate diffusion decoder into the training process and only update the adapter's parameters with the flow matching objective (Eq.(4)). To fully unlock the potential of the diffusion decoder for various generation tasks, we employ a diverse dataset comprising four different tasks: text-to-image, text-to-video, image editing, and video editing. Originally, the model was constrained to text-to-video synthesis. However, our multi-task training approach equips it with a broader range of capabilities, demonstrating enhanced generalization abilities.

Stage-3: Jointing finetuning for high-quality visual generation. To further improve the quality of generated visuals, we unfreeze and simultaneously fine-tune the vision head, adapter, and the diffusion decoder. During this stage, we incorporate higher-quality training data and increase the video sampling rate from 8 frames per second (fps) to 12 fps. Such adjustment is particularly advantageous for generating videos with substantial motion. Despite the increase in trainable parameters and a 50% rise in target frames, this phase does not significantly escalate the overall training cost. This efficiency is attributed to the solid generative foundation established in the previous stages, facilitating the effective optimization of generation quality.

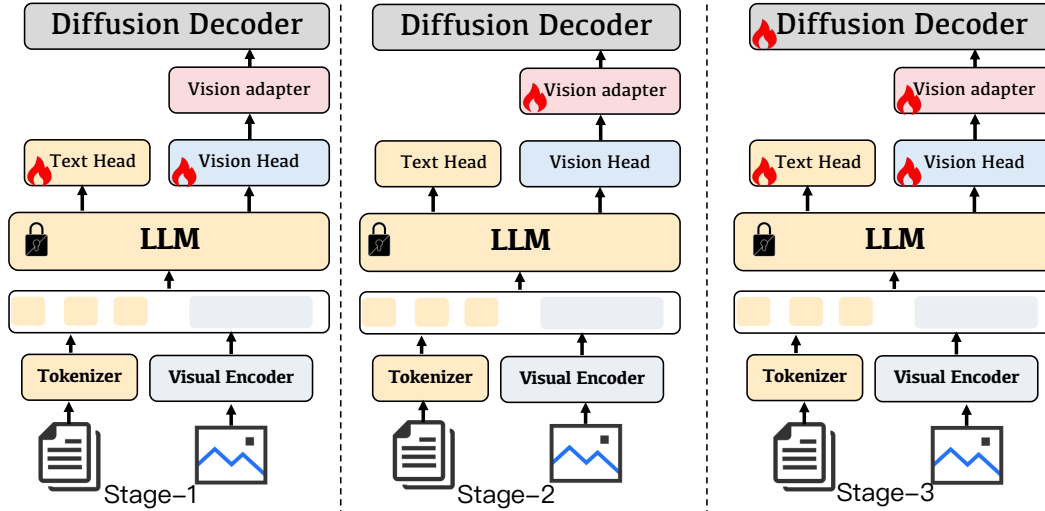


Figure 4: **Illustration of our multi-stages training strategy.** The flames denote the module parameters are trainable at each stage, and the block indicates that the model parameters are frozen.

Multi-task mixed training strategy. As mentioned earlier, our strategy involves multi-task training. While this approach can enhance generalization, it often slows down the convergence. To address this, we employ two acceleration strategies:

1. **Two-sub-stage multi-task Learning:** We organize the multi-task training into two distinct sub-stages. In the first sub-stage, training is focused exclusively on the text-to-image and text-to-video tasks. This method achieves two key objectives: it rapidly develops the model’s image generation capabilities and establishes a strong foundation for the later image editing and video editing tasks. In the second sub-stage, we incorporate all four tasks into joint training. By commencing the editing tasks from a well-initialized foundation, we facilitate faster convergence.
2. **Hybrid Mixed-Batching:** We employ a hybrid batching strategy tailored for different tasks and datasets. The training data is divided into two main groups: (1) video generation and editing, and (2) image generation and editing. For each group, batches are constructed separately, ensuring that data with the same resolution and frame count are processed together in a single forward and backward pass. This approach enhances computational efficiency. In contrast, a common alternative is to create separate batches for each individual task. Although this also permits multi-task learning within a single iteration, it can decrease the frequency of parameter updates for a given level of throughput (thereby maintaining high GPU utilization). Our hybrid strategy sustains high throughput while increasing the frequency of model updates, leading to faster convergence.

Think Mode. To endow our model with generative reasoning capabilities, we have developed a straightforward "thinking" mode. In this mode, the MLLM first performs a "reasoning rewrite" on the input prompt. Concurrently, it adjusts the output of the Vision Head to align with the rewritten prompt. Consequently, the diffusion model can generate an image or a video based on this new rewritten prompt and its corresponding Vision Head output. This thinking mode effectively leverages the advanced reasoning capabilities of the MLLM model to achieve reasoning-based generation, all without necessitating any retraining of the diffusion model.

Memory optimization and acceleration. We employ several techniques to optimize memory usage and expedite training. To minimize the memory footprint, we utilize DeepSpeed’s optimizer partitioning along with the ZeRO Stage-1 strategy.

Additionally, our multi-task configuration leads to longer conditioning sequences due to the inclusion of tokens from a 3D VAE encoding of the source video. To manage this, we use sequence parallelism to distribute the memory load across multiple GPUs. Lastly, gradient checkpointing is implemented

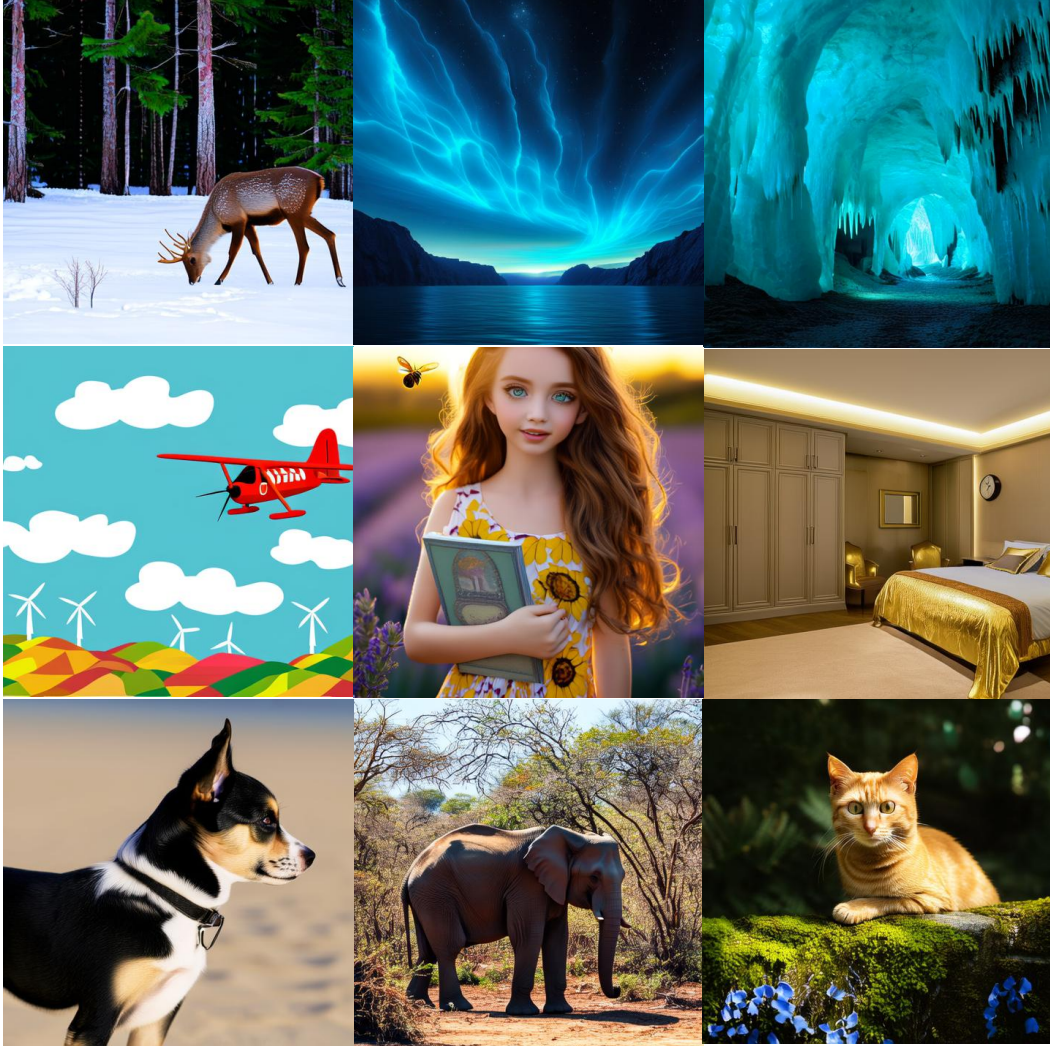


Figure 5: Example images generated by our proposed *Omni-Video* on text-to-image settings.

to reduce memory consumption from activations, especially when training with higher-resolution data.

5 Experiments

5.1 Experiment Settings

We employed distinct hyperparameter configurations for different tasks. For all generative tasks, we adopted the UniPC sampling strategy and utilized classifier-free guidance (CFG). The CFG scale is set as 5.0 for text-to-image generation tasks and 3.0 for text-to-video generation tasks, and the sampling steps are 50 for the former and 40 for the latter. Additionally, we use a universal negative prompt instead of a null condition to enhance output quality across all generative tasks. Regarding visual understanding, a top-p sampling strategy of 0.6 was applied to control diversity, alongside a temperature of 0.2 to manage randomness. The maximum number of new tokens generated was set to 1024. Moreover, the prompts used in our evaluation are given in the appendix.

Table 2: Performance Comparison on text-to-image benchmark GenEval.

Method	Params	Single Obj.	Two Obj.	Count.	Colors	Pos.	Color Attri.	Overall
SDv1.5 [7]	0.9B	0.97	0.38	0.35	0.76	0.04	0.06	0.43
SDv2.1 [7]	0.9B	0.98	0.51	0.44	0.85	0.07	0.17	0.50
SDXL [4]	2.6B	0.98	0.74	0.39	0.85	0.15	0.23	0.55
PixArt- α [89]	0.6B	0.98	0.50	0.44	0.80	0.08	0.07	0.48
DALL-E 2 [68]	6.5B	0.94	0.66	0.49	0.77	0.10	0.19	0.52
DALL-E 3 [3]	-	0.96	0.87	0.47	0.83	0.43	0.45	0.67
Chameleon [26]	34B	-	-	-	-	-	-	0.39
LWM [90]	7B	0.93	0.41	0.46	0.79	0.09	0.15	0.47
SEED-X \dagger [91]	17B	0.97	0.58	0.26	0.80	0.19	0.14	0.49
Show-o [28]	1.3B	0.95	0.52	0.49	0.82	0.11	0.28	0.53
JanusFlow [92]	1.3B	0.97	0.59	0.45	0.83	0.53	0.42	0.63
Ours	11B	0.93	0.52	0.51	0.67	0.10	0.20	0.49

5.2 Experiment Results

Performance on GenEval benchmark We evaluated our model’s visual generation performance on the GenEval benchmark. It is crucial to note a significant discrepancy between our training data and the prompts used in GenEval. Our model was trained on prompts rich in detail, whereas GenEval exclusively uses very short prompts for testing. We did not perform any special fine-tuning to address this domain gap. Despite this, our model achieved performance comparable to most state-of-the-art unified models on GenEval, as shown in 2. It is important to emphasize that previous unified models have primarily focused on the understanding and generation of images, whereas our work extends this paradigm to the video domain.

Text-to-Image results. Fig. 5 presents the qualitative results of our *Omni-Video* on text-to-image generation tasks. We can observe that the generated images exhibit remarkable visual fidelity across diverse domains, including human portraits, animals, and landscapes. For human faces, *Omni-Video* produces high-resolution details such as realistic skin textures and nuanced expressions. In animal depictions, intricate features like fur patterns and feather details are vividly rendered. Additionally, landscape generations showcase natural lighting effects and coherent structural compositions without artifacts.



Figure 6: Example video sequences generated by our proposed *Omni-Video* on text-to-video settings.

Text-to-Video results. Fig. 6 shows the qualitative results of our *Omni-Video* on text-to-video generation tasks, indicating our model’s ability to produce temporally coherent and dynamically

rich outputs. For instance, samples from the first-row samples demonstrate fine-grained facial performance: micro-expressions like orbicularis oculi contractions during laughter are captured with anatomical accuracy, while the camera’s lateral dolly motion maintains subject framing without introducing judder. Moreover, second-row footage achieves animal-specific locomotion realism—the rabbit exhibits proper quadrupedal gallop dynamics (suspensory phase clarity) alongside environment-reactive fur movement, with fog interaction showing consistent volumetric lighting transitions. Additionally, third-row sequences highlight complex urban reflections: synchronized footstep splashes create plausible ripples in the puddle, and the low-angle tracking shot preserves silhouette continuity between pedestrians despite varying stride lengths.

Image-to-Image editing. In addition to traditional text-to-image/video tasks, we further extend our *Omni-Video* to support detail-preserving image and video editing tasks. The qualitative results of image-to-image editing are illustrated in Fig. 7. For each row, the leftmost represents the source image provided, and the middle column are the ground truth, the rightmost images are edited output from our model. As shown in the first row, our method successfully introduces dynamic botanical elements while meticulously preserving structural integrity—notice the cactus spine details remain sharp even as a hyper-realistic bloom emerges from the center. The second-row samples demonstrate robust cross-domain style translation: the original mountain landscape retains its topographical accuracy even after transitions to anime aesthetics and futuristic environments, with snow textures maintaining consistency across stylistic shifts.

Furthermore, in the sky editing sequences (third row), our system achieves seamless temporal coherence in atmospheric transitions—cloud formations maintain continuity from overcast to dusk states, while the horizon line stays geometrically consistent as hues shift between magenta and indigo gradients. Finally, the lake edits (bottom row) exhibit precise perspective-aware expansion: the shorelines extend naturally under varying angles, and the water surface tension adapts authentically to different lighting conditions (midday azimuth vs. twilight reflections), without introducing tessellation artifacts.

Video-to-Video editing. Regarding video-to-video editing, the qualitative results presented in Fig. 8 demonstrate *Omni-Video*’s versatile adaptability across diverse spatiotemporal manipulation tasks. Obviously, our framework uniformly supports object removal, background replacement, attribute addition, *etc.*, while maintaining cross-frame consistency. For instance, the background of the old man is changed from street to an ocean, the man besides the woman (people and grasses on the beach) is removed, and a hat is added to the woman in Fig. 8. Crucially, these compound edits preserve microscopic details with no flickering in edited regions and wind-responsive elements, achieving a cross-frame consistency score that underscores the method’s unified adaptability for complex multi-operation editing scenarios.

Video understanding. Furthermore, we evaluate the video understanding performance of our *Omni-Video* in Fig. 9, where the system demonstrates robust multimodal reasoning across diverse spatiotemporal contexts. In the Pleistocene snowscape sequence, it accurately grounds quantitative analysis ("two mammoths") while distinguishing species-specific traits ("brownish elephant with tusks") and inferring motion dynamics (animal approaching the camera). For the companion winter scene featuring golden retriever puppies, the method identifies seasonal context ("winter, as indicated by snow cover") and derives emotional valence ("joy and happiness") from behavioral cues (playful rolling, social interaction), even when occlusions occur during rapid canine movements. These results underscore *Omni-Video*’s ability to simultaneously process object attributes, temporal action patterns, and environmental metadata—key competencies for unified video grounding and interpretation. The consistent performance across paleontological and domestic contexts highlights its domain-agnostic adaptability.

Think mode. Finally, Fig. 10 present the videos produced by our system under "think" mode, in which the model is asked to "think" with a long chain-of-thought to fully understand user instructions and produce corresponding visual output. For example, when generating the mausoleum sequence, our model first parses ambiguous descriptors—interpreting "elegant marble" as requiring stratified erosion textures and "Indian architectural brilliance" as necessitating precise dome geometry—before translating these inferences into optimized visual tokens. This manifests as calibrated material

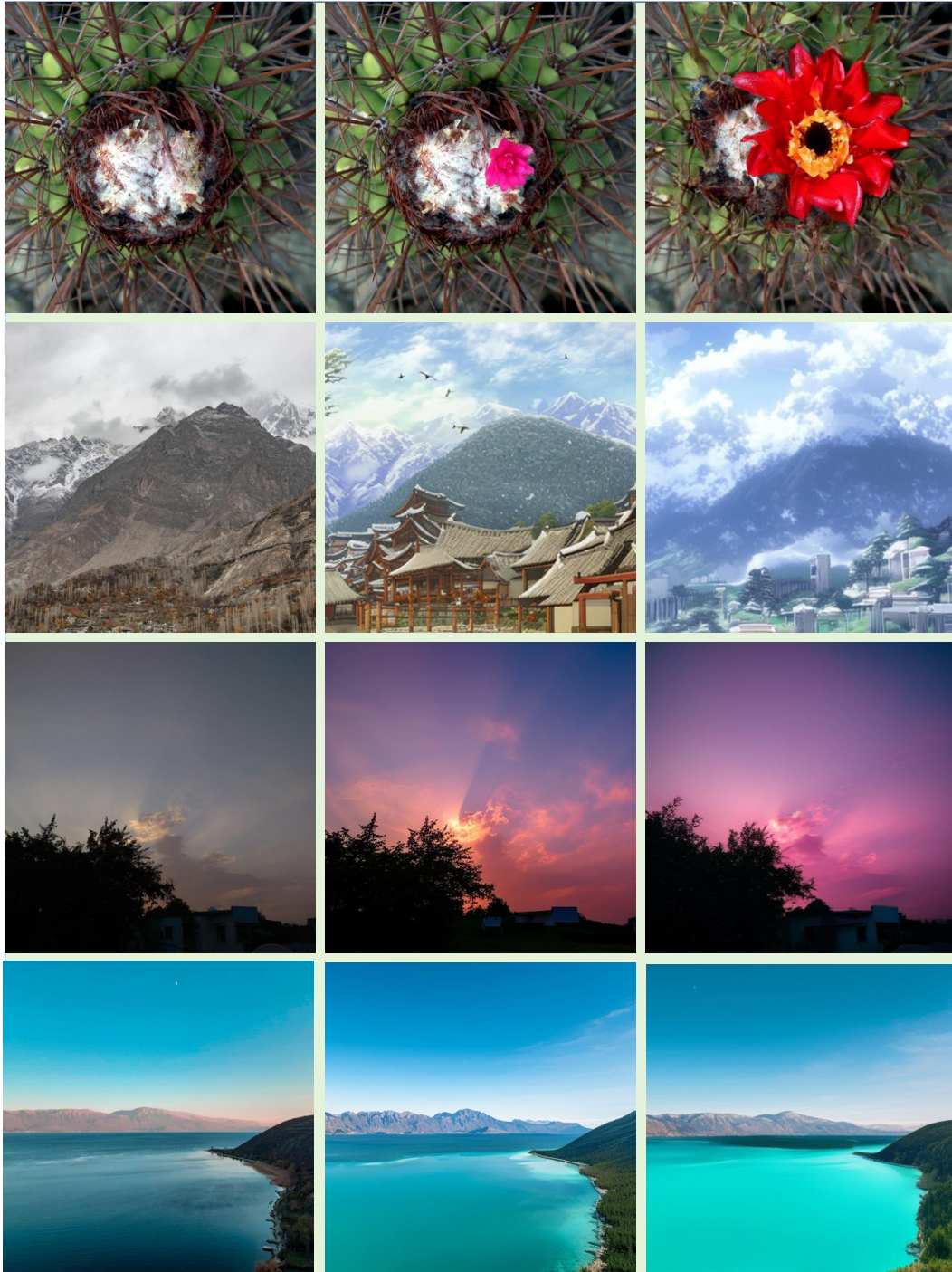


Figure 7: **Example edited images generated by our proposed *Omni-Video* on image-to-image editing settings.** For each row, the leftmost represents the source image provided, and the middle column is the ground truth, the rightmost image is the edited output from our model.

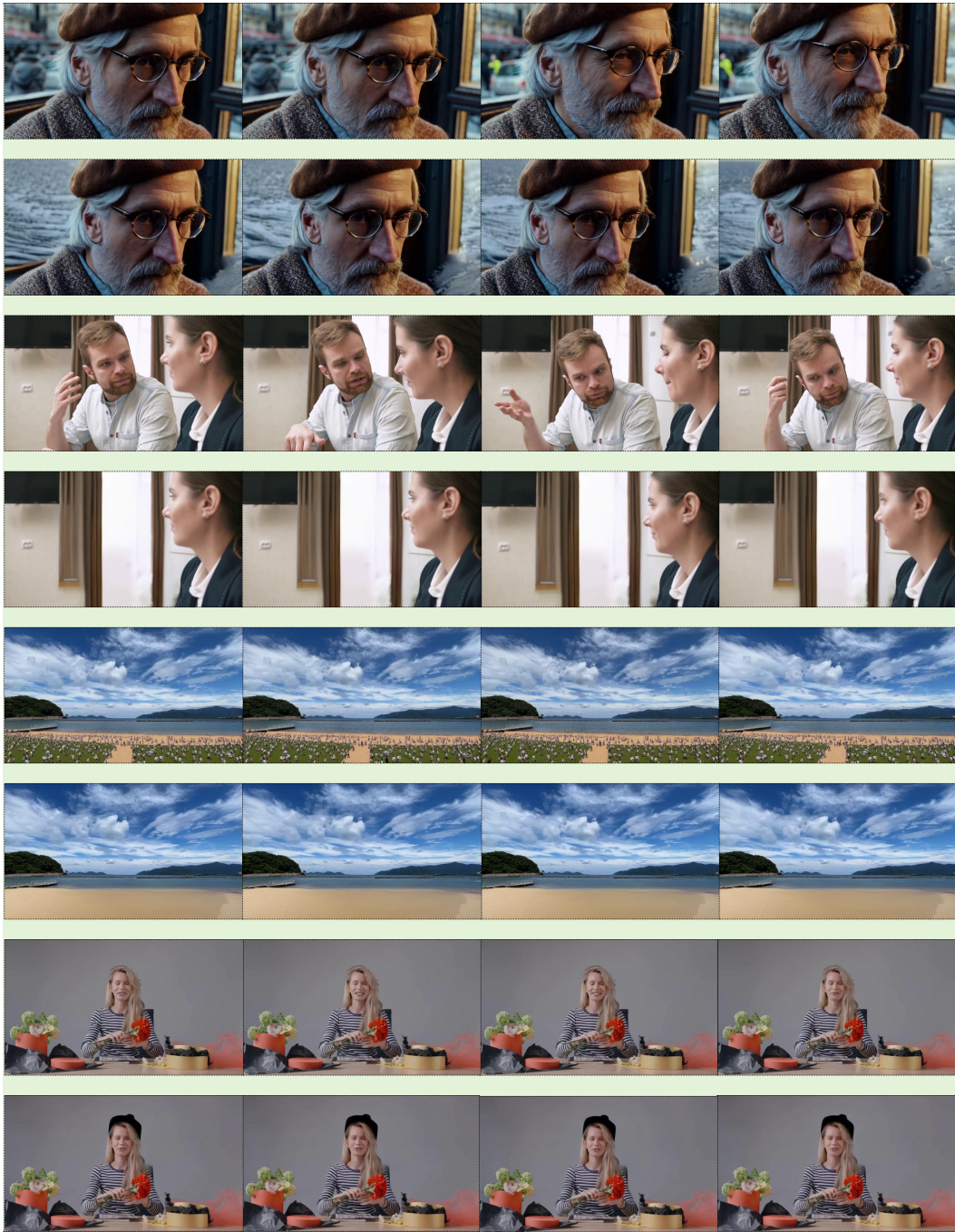


Figure 8: **Example edited videos generated by our proposed *Omni-Video* on video-to-video editing settings.** For each pair, the upper one represents the source videos provided by users, and bottom videos are edited output from our model.

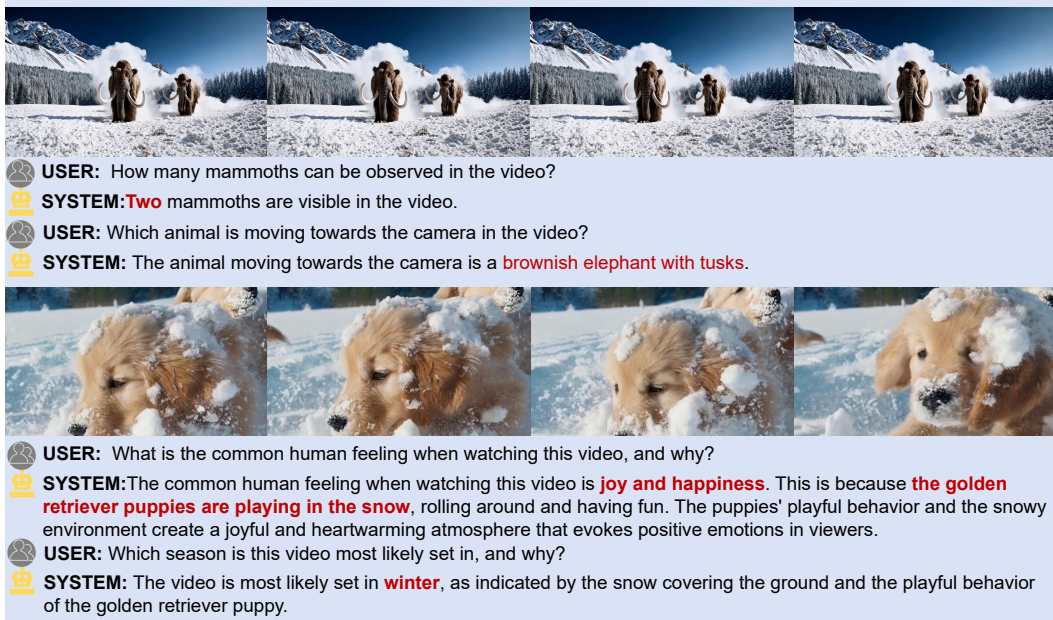


Figure 9: Example responses generated by our proposed *Omni-Video* on video understanding settings.

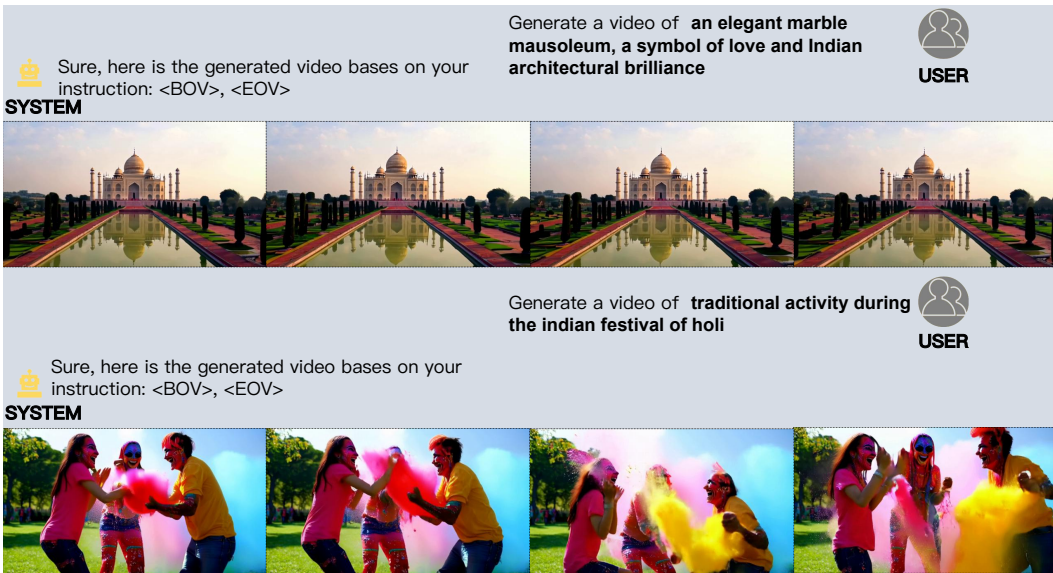


Figure 10: Example videos generated by our proposed *Omni-Video* under *think mode* for text-to-video tasks that require thinking with user instructions.

properties (light refraction indices in marble veins), architecturally accurate proportions (minaret height-to-width ratios), and environmentally responsive details (wind-aligned water ripples).

6 Limitations

Despite successfully unifying video understanding, generation and editing in a single framework via connecting MLLMs with diffusion decoder, our approach faces persistent limitations rooted in data scalability, computational constraints, and architectural fragmentation. The current implementation struggles with high-fidelity, long-duration video synthesis due to prohibitive memory demands and limited training data for complex interactions and distribution modeling. More fundamentally, the decoupled design between diffusion decoders and MLLMs creates optimization misalignments of latent representations optimized for generative tasks fail to seamlessly transfer to discriminative understanding tasks, particularly in video domains requiring frame-by-frame causal reasoning. We plan to continuously address these limitations through systematic enhancements to our framework. Ongoing efforts might include refining the diffusion-MLLM interface via shared optimization, developing adaptive training protocols for complex physical interactions, and scalable data curation pipelines to gather higher-quality training data.

References

- [1] Zhe Chen, Jiannan Wu, Wenhai Wang, Weijie Su, Guo Chen, Sen Xing, Muyan Zhong, Qinglong Zhang, Xizhou Zhu, Lewei Lu, et al. Internvl: Scaling up vision foundation models and aligning for generic visual-linguistic tasks. In *Proceedings of the IEEE/CVF conference on computer vision and pattern recognition*, pages 24185–24198, 2024.
- [2] Shuai Bai, Keqin Chen, Xuejing Liu, Jialin Wang, Wenbin Ge, Sibao Song, Kai Dang, Peng Wang, Shijie Wang, Jun Tang, et al. Qwen2. 5-vl technical report. *arXiv preprint arXiv:2502.13923*, 2025.
- [3] James Betker, Gabriel Goh, Li Jing, Tim Brooks, Jianfeng Wang, Linjie Li, Long Ouyang, Juntang Zhuang, Joyce Lee, Yufei Guo, et al. Improving image generation with better captions. <https://openai.com/dall-e-3>, 2023.
- [4] Dustin Podell, Zion English, Kyle Lacey, Andreas Blattmann, Tim Dockhorn, Jonas Müller, Joe Penna, and Robin Rombach. Sdxl: Improving latent diffusion models for high-resolution image synthesis. *arXiv preprint arXiv:2307.01952*, 2023.
- [5] Team Wan, Ang Wang, Baole Ai, Bin Wen, Chaojie Mao, Chen-Wei Xie, Di Chen, Feiwu Yu, Haiming Zhao, Jianxiao Yang, et al. Wan: Open and advanced large-scale video generative models. *arXiv preprint arXiv:2503.20314*, 2025.
- [6] Joseph Redmon, Santosh Divvala, Ross Girshick, and Ali Farhadi. You only look once: Unified, real-time object detection. In *Proceedings of the IEEE conference on computer vision and pattern recognition*, pages 779–788, 2016.
- [7] Robin Rombach, Andreas Blattmann, Dominik Lorenz, Patrick Esser, and Björn Ommer. High-resolution image synthesis with latent diffusion models. In *Proceedings of the IEEE/CVF conference on computer vision and pattern recognition*, pages 10684–10695, 2022.
- [8] Kaiming He, Xiangyu Zhang, Shaoqing Ren, and Jian Sun. Deep residual learning for image recognition. In *Proceedings of the IEEE conference on computer vision and pattern recognition*, pages 770–778, 2016.
- [9] Alexey Dosovitskiy, Lucas Beyer, Alexander Kolesnikov, Dirk Weissenborn, Xiaohua Zhai, Thomas Unterthiner, Mostafa Dehghani, Matthias Minderer, Georg Heigold, Sylvain Gelly, et al. An image is worth 16x16 words: Transformers for image recognition at scale. In *International Conference on Learning Representations*.
- [10] Jacob Devlin, Ming-Wei Chang, Kenton Lee, and Kristina Toutanova. Bert: Pre-training of deep bidirectional transformers for language understanding. In *Proceedings of the 2019 conference of the North American chapter of the association for computational linguistics: human language technologies, volume 1 (long and short papers)*, pages 4171–4186, 2019.

- [11] Tom Brown, Benjamin Mann, Nick Ryder, Melanie Subbiah, Jared D Kaplan, Prafulla Dhariwal, Arvind Neelakantan, Pranav Shyam, Girish Sastry, Amanda Askell, et al. Language models are few-shot learners. *Advances in neural information processing systems*, 33:1877–1901, 2020.
- [12] Colin Raffel, Noam Shazeer, Adam Roberts, Katherine Lee, Sharan Narang, Michael Matena, Yanqi Zhou, Wei Li, and Peter J Liu. Exploring the limits of transfer learning with a unified text-to-text transformer. *Journal of machine learning research*, 21(140):1–67, 2020.
- [13] Alexei Baevski, Yuhao Zhou, Abdelrahman Mohamed, and Michael Auli. wav2vec 2.0: A framework for self-supervised learning of speech representations. *Advances in neural information processing systems*, 33:12449–12460, 2020.
- [14] Sander Dieleman, Heiga Zen, Karen Simonyan, Oriol Vinyals, Alex Graves, Nal Kalchbrenner, Andrew Senior, Koray Kavukcuoglu, et al. Wavenet: A generative model for raw audio. *arXiv preprint arXiv:1609.03499*, 12, 2016.
- [15] Daniel S Park, William Chan, Yu Zhang, Chung-Cheng Chiu, Barret Zoph, Ekin D Cubuk, and Quoc V Le. Specaugment: A simple data augmentation method for automatic speech recognition. *Interspeech 2019*, page 2613, 2019.
- [16] Alec Radford, Jong Wook Kim, Tao Xu, Greg Brockman, Christine McLeavey, and Ilya Sutskever. Robust speech recognition via large-scale weak supervision. In *International conference on machine learning*, pages 28492–28518. PMLR, 2023.
- [17] Xiaokang Chen, Zhiyu Wu, Xingchao Liu, Zizheng Pan, Wen Liu, Zhenda Xie, Xingkai Yu, and Chong Ruan. Janus-pro: Unified multimodal understanding and generation with data and model scaling. *arXiv preprint arXiv:2501.17811*, 2025.
- [18] Shengbang Tong, David Fan, Jiachen Zhu, Yunyang Xiong, Xinlei Chen, Koustuv Sinha, Michael Rabbat, Yann LeCun, Saining Xie, and Zhuang Liu. Metamorph: Multimodal understanding and generation via instruction tuning. *arXiv preprint arXiv:2412.14164*, 2024.
- [19] Tao Wang, Cong Zhang, Xingguang Qu, Kun Li, Weiwei Liu, and Chang Huang. Diffad: A unified diffusion modeling approach for autonomous driving. *arXiv preprint arXiv:2503.12170*, 2025.
- [20] Yi-Min Chou, Yi-Ming Chan, Jia-Hong Lee, Chih-Yi Chiu, and Chu-Song Chen. Unifying and merging well-trained deep neural networks for inference stage. In *Proceedings of the 27th International Joint Conference on Artificial Intelligence*, pages 2049–2056, 2018.
- [21] Ronghang Hu and Amanpreet Singh. Unit: Multimodal multitask learning with a unified transformer. In *Proceedings of the IEEE/CVF international conference on computer vision*, pages 1439–1449, 2021.
- [22] Haiyang Wang, Hao Tang, Li Jiang, Shaoshuai Shi, Muhammad Ferjad Naeem, Hongsheng Li, Bernt Schiele, and Liwei Wang. Git: Towards generalist vision transformer through universal language interface. In *European Conference on Computer Vision*, pages 55–73. Springer, 2024.
- [23] Jiu-hai Chen, Zhiyang Xu, Xichen Pan, Yushi Hu, Can Qin, Tom Goldstein, Lifu Huang, Tianyi Zhou, Saining Xie, Silvio Savarese, et al. Blip3-o: A family of fully open unified multimodal models-architecture, training and dataset. *arXiv preprint arXiv:2505.09568*, 2025.
- [24] Chaorui Deng, Deyao Zhu, Kunchang Li, Chenhui Gou, Feng Li, Zeyu Wang, Shu Zhong, Weihao Yu, Xiaonan Nie, Ziang Song, et al. Emerging properties in unified multimodal pretraining. *arXiv preprint arXiv:2505.14683*, 2025.
- [25] Xinlong Wang, Xiaosong Zhang, Zhengxiong Luo, Quan Sun, Yufeng Cui, Jinsheng Wang, Fan Zhang, Yueze Wang, Zhen Li, Qiying Yu, et al. Emu3: Next-token prediction is all you need. *arXiv preprint arXiv:2409.18869*, 2024.
- [26] Chameleon Team. Chameleon: Mixed-modal early-fusion foundation models. *arXiv preprint arXiv:2405.09818*, 2024.

- [27] Chunting Zhou, Lili Yu, Arun Babu, Kushal Tirumala, Michihiro Yasunaga, Leonid Shamis, Jacob Kahn, Xuezhe Ma, Luke Zettlemoyer, and Omer Levy. Transfusion: Predict the next token and diffuse images with one multi-modal model. *arXiv preprint arXiv:2408.11039*, 2024.
- [28] Jinheng Xie, Weijia Mao, Zechen Bai, David Junhao Zhang, Weihao Wang, Kevin Qinghong Lin, Yuchao Gu, Zhijie Chen, Zhenheng Yang, and Mike Zheng Shou. Show-o: One single transformer to unify multimodal understanding and generation. *arXiv preprint arXiv:2408.12528*, 2024.
- [29] Ji Lin, Hongxu Yin, Wei Ping, Pavlo Molchanov, Mohammad Shoeybi, and Song Han. Vila: On pre-training for visual language models. In *Proceedings of the IEEE/CVF Conference on Computer Vision and Pattern Recognition*, pages 26689–26699, 2024.
- [30] Michael Tschannen, Alexey Gritsenko, Xiao Wang, Muhammad Ferjad Naeem, Ibrahim Alabdulmohsin, Nikhil Parthasarathy, Talfan Evans, Lucas Beyer, Ye Xia, Basil Mustafa, et al. Siglip 2: Multilingual vision-language encoders with improved semantic understanding, localization, and dense features. *arXiv preprint arXiv:2502.14786*, 2025.
- [31] Yongsheng Yu, Ziyun Zeng, Hang Hua, Jianlong Fu, and Jiebo Luo. Promptfix: You prompt and we fix the photo. *arXiv preprint arXiv:2405.16785*, 2024.
- [32] Haozhe Zhao, Xiaojian Shawn Ma, Liang Chen, Shuzheng Si, Rujie Wu, Kaikai An, Peiyu Yu, Minjia Zhang, Qing Li, and Baobao Chang. Ultraedit: Instruction-based fine-grained image editing at scale. *Advances in Neural Information Processing Systems*, 37:3058–3093, 2024.
- [33] Shu Zhang, Xinyi Yang, Yihao Feng, Can Qin, Chia-Chih Chen, Ning Yu, Zeyuan Chen, Huan Wang, Silvio Savarese, Stefano Ermon, et al. Hive: Harnessing human feedback for instructional visual editing. In *Proceedings of the IEEE/CVF Conference on Computer Vision and Pattern Recognition*, pages 9026–9036, 2024.
- [34] Josh Achiam, Steven Adler, Sandhini Agarwal, Lama Ahmad, Ilge Akkaya, Florencia Leoni Aleman, Diogo Almeida, Janko Altenschmidt, Sam Altman, Shyamal Anadkat, et al. Gpt-4 technical report. *arXiv preprint arXiv:2303.08774*, 2023.
- [35] Aaron Grattafiori, Abhimanyu Dubey, Abhinav Jauhri, Abhinav Pandey, Abhishek Kadian, Ahmad Al-Dahle, Aiesha Letman, Akhil Mathur, Alan Schelten, Alex Vaughan, et al. The llama 3 herd of models. *arXiv preprint arXiv:2407.21783*, 2024.
- [36] An Yang, Anfeng Li, Baosong Yang, Beichen Zhang, Binyuan Hui, Bo Zheng, Bowen Yu, Chang Gao, Chengen Huang, Chenxu Lv, et al. Qwen3 technical report. *arXiv preprint arXiv:2505.09388*, 2025.
- [37] Bo Li, Yuanhan Zhang, Dong Guo, Renrui Zhang, Feng Li, Hao Zhang, Kaichen Zhang, Peiyuan Zhang, Yanwei Li, Ziwei Liu, et al. Llava-onevision: Easy visual task transfer. *arXiv preprint arXiv:2408.03326*, 2024.
- [38] Dong Guo, Faming Wu, Feida Zhu, Fuxing Leng, Guang Shi, Haobin Chen, Haoqi Fan, Jian Wang, Jianyu Jiang, Jiawei Wang, et al. Seed1. 5-vl technical report. *arXiv preprint arXiv:2505.07062*, 2025.
- [39] Alec Radford, Jong Wook Kim, Chris Hallacy, Aditya Ramesh, Gabriel Goh, Sandhini Agarwal, Girish Sastry, Amanda Askell, Pamela Mishkin, Jack Clark, et al. Learning transferable visual models from natural language supervision. In *International conference on machine learning*, pages 8748–8763. PmLR, 2021.
- [40] Haotian Liu, Chunyuan Li, Qingyang Wu, and Yong Jae Lee. Visual instruction tuning. *Advances in neural information processing systems*, 36:34892–34916, 2023.
- [41] Haotian Liu, Chunyuan Li, Yuheng Li, and Yong Jae Lee. Improved baselines with visual instruction tuning. In *Proceedings of the IEEE/CVF Conference on Computer Vision and Pattern Recognition*, pages 26296–26306, 2024.

- [42] Deyao Zhu, Jun Chen, Xiaoqian Shen, Xiang Li, and Mohamed Elhoseiny. Minigpt-4: Enhancing vision-language understanding with advanced large language models. *arXiv preprint arXiv:2304.10592*, 2023.
- [43] Peng Wang, Shuai Bai, Sinan Tan, Shijie Wang, Zhihao Fan, Jinze Bai, Keqin Chen, Xuejing Liu, Jialin Wang, Wenbin Ge, et al. Qwen2-vl: Enhancing vision-language model’s perception of the world at any resolution. *arXiv preprint arXiv:2409.12191*, 2024.
- [44] Albert Q Jiang, Alexandre Sablayrolles, Antoine Roux, Arthur Mensch, Blanche Savary, Chris Bamford, Devendra Singh Chaplot, Diego de las Casas, Emma Bou Hanna, Florian Bressand, et al. Mixtral of experts. *arXiv preprint arXiv:2401.04088*, 2024.
- [45] Aixin Liu, Bei Feng, Bin Wang, Bingxuan Wang, Bo Liu, Chenggang Zhao, Chengqi Deng, Chong Ruan, Damai Dai, Daya Guo, et al. Deepseek-v2: A strong, economical, and efficient mixture-of-experts language model. *arXiv preprint arXiv:2405.04434*, 2024.
- [46] Junnan Li, Dongxu Li, Silvio Savarese, and Steven Hoi. Blip-2: Bootstrapping language-image pre-training with frozen image encoders and large language models. In *International conference on machine learning*, pages 19730–19742. PMLR, 2023.
- [47] Jean-Baptiste Alayrac, Jeff Donahue, Pauline Luc, Antoine Miech, Iain Barr, Yana Hasson, Karel Lenc, Arthur Mensch, Katherine Millican, Malcolm Reynolds, et al. Flamingo: a visual language model for few-shot learning. *Advances in neural information processing systems*, 35:23716–23736, 2022.
- [48] Siddharth Karamcheti, Suraj Nair, Ashwin Balakrishna, Percy Liang, Thomas Kollar, and Dorsa Sadigh. Prismatic vlms: Investigating the design space of visually-conditioned language models. In *Forty-first International Conference on Machine Learning*, 2024.
- [49] Ian J Goodfellow, Jean Pouget-Abadie, Mehdi Mirza, Bing Xu, David Warde-Farley, Sherjil Ozair, Aaron Courville, and Yoshua Bengio. Generative adversarial nets. *Advances in neural information processing systems*, 27, 2014.
- [50] Jonathan Ho, Ajay Jain, and Pieter Abbeel. Denoising diffusion probabilistic models. *Advances in neural information processing systems*, 33:6840–6851, 2020.
- [51] George E.P. Box, Gwilym M. Jenkins, and Gregory C. Reinsel. *Time Series Analysis: Forecasting and Control*. Holden-Day, 1970.
- [52] Alec Radford, Karthik Narasimhan, Tim Salimans, Ilya Sutskever, et al. Improving language understanding by generative pre-training.(2018), 2018.
- [53] Cheng Lu, Yuhao Zhou, Fan Bao, Jianfei Chen, Chongxuan Li, and Jun Zhu. Dpm-solver: A fast ode solver for diffusion probabilistic model sampling in around 10 steps. *Advances in Neural Information Processing Systems*, 35:5775–5787, 2022.
- [54] Tero Karras, Miika Aittala, Jaakko Lehtinen, Janne Hellsten, Timo Aila, and Samuli Laine. Analyzing and improving the training dynamics of diffusion models. In *Proceedings of the IEEE/CVF Conference on Computer Vision and Pattern Recognition*, pages 24174–24184, 2024.
- [55] Yu Gao, Lixue Gong, Qiushan Guo, Xiaoxia Hou, Zhichao Lai, Fanshi Li, Liang Li, Xiaochen Lian, Chao Liao, Liyang Liu, et al. Seedream 3.0 technical report. *arXiv preprint arXiv:2504.11346*, 2025.
- [56] Cheng Lu and Yang Song. Simplifying, stabilizing and scaling continuous-time consistency models. *arXiv preprint arXiv:2410.11081*, 2024.
- [57] Yang Song and Prafulla Dhariwal. Improved techniques for training consistency models. *arXiv preprint arXiv:2310.14189*, 2023.
- [58] Bingchen Liu, Ehsan Akhgari, Alexander Visheratin, Aleks Kamko, Linmiao Xu, Shivam Shrirao, Chase Lambert, Joao Souza, Suhail Doshi, and Daiqing Li. Playground v3: Improving text-to-image alignment with deep-fusion large language models. *arXiv preprint arXiv:2409.10695*, 2024.

- [59] William Peebles and Saining Xie. Scalable diffusion models with transformers. In *Proceedings of the IEEE/CVF international conference on computer vision*, pages 4195–4205, 2023.
- [60] OpenAI. Video generation models as world simulators. <https://openai.com/index/video-generation-models-as-world-simulators/>, 2024. Accessed: 2025-07-06.
- [61] Zangwei Zheng, Xiangyu Peng, Tianji Yang, Chenhui Shen, Shenggui Li, Hongxin Liu, Yukun Zhou, Tianyi Li, and Yang You. Open-sora: Democratizing efficient video production for all. *arXiv preprint arXiv:2412.20404*, 2024.
- [62] Zhiyu Tan, Junyan Wang, Hao Yang, Luozheng Qin, Hesen Chen, Qiang Zhou, and Hao Li. Raccoon: Multi-stage diffusion training with coarse-to-fine curating videos. *arXiv preprint arXiv:2502.21314*, 2025.
- [63] Kling AI. Kling ai: Next-gen ai video & ai image generator. <https://app.klingai.com/global/>, 2024. Accessed: 2025-07-06.
- [64] Yu Gao, Haoyuan Guo, Tuyen Hoang, Weilin Huang, Lu Jiang, Fangyuan Kong, Huixia Li, Jiashi Li, Liang Li, Xiaojie Li, et al. Seedance 1.0: Exploring the boundaries of video generation models. *arXiv preprint arXiv:2506.09113*, 2025.
- [65] Lijun Yu, José Lezama, Nitesh B Gundavarapu, Luca Versari, Kihyuk Sohn, David Minnen, Yong Cheng, Vighnesh Birodkar, Agrim Gupta, Xiuye Gu, et al. Language model beats diffusion—tokenizer is key to visual generation. *arXiv preprint arXiv:2310.05737*, 2023.
- [66] Keyu Tian, Yi Jiang, Zehuan Yuan, Bingyue Peng, and Liwei Wang. Visual autoregressive modeling: Scalable image generation via next-scale prediction. *Advances in neural information processing systems*, 37:84839–84865, 2024.
- [67] Tianhong Li, Yonglong Tian, He Li, Mingyang Deng, and Kaiming He. Autoregressive image generation without vector quantization. *Advances in Neural Information Processing Systems*, 37:56424–56445, 2024.
- [68] Aditya Ramesh, Prafulla Dhariwal, Alex Nichol, Casey Chu, and Mark Chen. Hierarchical text-conditional image generation with clip latents. *arXiv preprint arXiv:2204.06125*, 2022.
- [69] Junfeng Wu, Yi Jiang, Chuofan Ma, Yuliang Liu, Hengshuang Zhao, Zehuan Yuan, Song Bai, and Xiang Bai. Liquid: Language models are scalable and unified multi-modal generators. *arXiv preprint arXiv:2412.04332*, 2025.
- [70] Chao Liao, Liyang Liu, Xun Wang, Zhengxiong Luo, Xinyu Zhang, Wenliang Zhao, Jie Wu, Liang Li, Zhi Tian, and Weilin Huang. Mogao: An omni foundation model for interleaved multi-modal generation. *arXiv preprint arXiv:2505.05472*, 2025.
- [71] Aaron Van Den Oord, Oriol Vinyals, et al. Neural discrete representation learning. *Advances in neural information processing systems*, 30, 2017.
- [72] Xiaohua Zhai, Basil Mustafa, Alexander Kolesnikov, and Lucas Beyer. Sigmoid loss for language image pre-training. In *Proceedings of the IEEE/CVF international conference on computer vision*, pages 11975–11986, 2023.
- [73] Peize Sun, Yi Jiang, Shoufa Chen, Shilong Zhang, Bingyue Peng, Ping Luo, and Zehuan Yuan. Autoregressive model beats diffusion: Llama for scalable image generation. *arXiv preprint arXiv:2406.06525*, 2024.
- [74] Lijie Fan, Luming Tang, Siyang Qin, Tianhong Li, Xuan Yang, Siyuan Qiao, Andreas Steiner, Chen Sun, Yuanzhen Li, Tao Zhu, et al. Unified autoregressive visual generation and understanding with continuous tokens. *arXiv preprint arXiv:2503.13436*, 2025.
- [75] Jinheng Xie, Zhenheng Yang, and Mike Zheng Shou. Show-o2: Improved native unified multimodal models. *arXiv preprint arXiv:2506.15564*, 2025.
- [76] Yaron Lipman, Ricky TQ Chen, Heli Ben-Hamu, Maximilian Nickel, and Matt Le. Flow matching for generative modeling. *arXiv preprint arXiv:2210.02747*, 2022.

- [77] Keqiang Sun, Junting Pan, Yuying Ge, Hao Li, Haodong Duan, Xiaoshi Wu, Renrui Zhang, Aojun Zhou, Zipeng Qin, Yi Wang, et al. Journeydb: A benchmark for generative image understanding. *Advances in neural information processing systems*, 36:49659–49678, 2023.
- [78] Lin Chen, Jinsong Li, Xiaoyi Dong, Pan Zhang, Conghui He, Jiaqi Wang, Feng Zhao, and Dahua Lin. Sharegpt4v: Improving large multi-modal models with better captions. In *European Conference on Computer Vision*, pages 370–387. Springer, 2024.
- [79] Peter Tong, Ellis Brown, Penghao Wu, Sanghyun Woo, Adithya Jairam Vedagiri IYER, Sai Charitha Akula, Shusheng Yang, Jihan Yang, Manoj Middepogu, Ziteng Wang, et al. Cambrian-1: A fully open, vision-centric exploration of multimodal llms. *Advances in Neural Information Processing Systems*, 37:87310–87356, 2024.
- [80] Wanrong Zhu, Jack Hessel, Anas Awadalla, Samir Yitzhak Gadre, Jesse Dodge, Alex Fang, Youngjae Yu, Ludwig Schmidt, William Yang Wang, and Yejin Choi. Multimodal c4: An open, billion-scale corpus of images interleaved with text. *Advances in Neural Information Processing Systems*, 36:8958–8974, 2023.
- [81] Yuanhan Zhang, Jinming Wu, Wei Li, Bo Li, Zejun Ma, Ziwei Liu, and Chunyuan Li. Video instruction tuning with synthetic data. *arXiv preprint arXiv:2410.02713*, 2024.
- [82] Orr Zohar, Xiaohan Wang, Yonatan Bitton, Idan Szpektor, and Serena Yeung-Levy. Video-star: Self-training enables video instruction tuning with any supervision. *arXiv preprint arXiv:2407.06189*, 2024.
- [83] Lin Chen, Xilin Wei, Jinsong Li, Xiaoyi Dong, Pan Zhang, Yuhang Zang, Zehui Chen, Haodong Duan, Zhenyu Tang, Li Yuan, et al. Sharegpt4video: Improving video understanding and generation with better captions. *Advances in Neural Information Processing Systems*, 37:19472–19495, 2024.
- [84] Christoph Schuhmann, Romain Beaumont, Richard Vencu, Cade Gordon, Ross Wightman, Mehdi Cherti, Theo Coombes, Aarush Katta, Clayton Mullis, Mitchell Wortsman, et al. Laion-5b: An open large-scale dataset for training next generation image-text models. *Advances in neural information processing systems*, 35:25278–25294, 2022.
- [85] Byeon Minwoo, Park Beomhee, Kim Haecheon, Lee Sungjun, Baek Woonhyuk, and Kim Saehoon. Coyo-700m: Image-text pair dataset. <https://github.com/kakaobrain/coyo-dataset>, 2022.
- [86] Hongwei Xue, Tiankai Hang, Yanhong Zeng, Yuchong Sun, Bei Liu, Huan Yang, Jianlong Fu, and Baining Guo. Advancing high-resolution video-language representation with large-scale video transcriptions. In *Proceedings of the IEEE/CVF Conference on Computer Vision and Pattern Recognition*, pages 5036–5045, 2022.
- [87] Qifan Yu, Wei Chow, Zhongqi Yue, Kaihang Pan, Yang Wu, Xiaoyang Wan, Juncheng Li, Siliang Tang, Hanwang Zhang, and Yueting Zhuang. Anyedit: Mastering unified high-quality image editing for any idea. *arXiv preprint arXiv:2411.15738*, 2024.
- [88] Bojia Zi, Penghui Ruan, Marco Chen, Xianbiao Qi, Shaozhe Hao, Shihao Zhao, Youze Huang, Bin Liang, Rong Xiao, and Kam-Fai Wong. Se²norita-2m: A high-quality instruction-based dataset for general video editing by video specialists. *arXiv preprint arXiv:2502.06734*, 2025.
- [89] Jingye Chen, Jiajun Yu, Changqian Ge, Liang Yao, Erfei Xie, Yichun Wu, Zhiqi Wang, Joe Kwok, Ping Luo, Haiming Lu, et al. Pixart-alpha: Fast training of diffusion transformer for photorealistic text-to-image synthesis. *arXiv preprint arXiv:2310.00426*, 2023.
- [90] Hao Liu, Wenjie Yan, Matei Zaharia, and Pieter Abbeel. World model on million-length video and language with ringattention. *arXiv preprint arXiv:2402.08268*, 2024.
- [91] Yuying Ge, Sijie Zhao, Jinguo Zhu, Yixiao Ge, Kun Yi, Lin Song, Chen Li, Xiaohan Ding, and Ying Shan. Seed-x: Multimodal models with unified multi-granularity comprehension and generation. *arXiv preprint arXiv:2404.14396*, 2024.

- [92] Wenbo Ma, Xintao Wang, Chao Li, Guanzhong Wang, Haofan Wang, Yanpeng Liu, Zhaokang Chen, Yaohui Wang, Xiaoyang Kang, and Limin Wang. Janusflow: Harmonizing autoregression and rectified flow for unified multimodal understanding and generation. In *Proceedings of the IEEE/CVF Conference on Computer Vision and Pattern Recognition (CVPR)*, 2025.

A Prompts Used in the Main Text

Here we list all the prompts used in the main text. The prompts are arranged in the order of their appearance in the figure, from top to bottom and from left to right.

Prompts used in Figure 1

Text-to-Image:

- p1: A volcanic springs steaming in Icelandic winters. Azure pools steam among obsidian rocks where snowflakes vanish near bubbling geothermal vents.
- p2: A serene scene of a misty morning in a valley, with a calm river flowing through it. The sunlight is shining through the trees, casting a warm glow on the landscape. The river is surrounded by lush green trees and a forest, creating a peaceful atmosphere.
- p3: An image features Finnish icebreaker ships plowing Arctic channels. Steel prows split blue-white plates forming frozen wakes under polar twilight streaked with sun dogs.
- p4: A black and white photograph of a serene mountain lake surrounded by trees. The mountain can be seen in the distance, towering over the lake. The reflection of the mountain and its snowy peak can be seen clearly in the calm waters of the lake.
- p5: Antarctic icebergs sculpted by polar winds. Azure caverns glow in monumental ice cliffs floating through silver seas where penguins porpoise through waves.
- p6: A futuristic image featuring a woman with glowing yellow eyes. She is wearing a black and gold outfit, which is adorned with intricate patterns and lights. The woman has long hair, and her eyes are prominently glowing yellow. She is the main focus of the scene.
- p7: An image that captures the essence of retro chic. At the center of the frame is a woman exuding a sense of confidence and style.
- p8: An image depicts a dystopian, cyberpunk-inspired scene. In the foreground, a figure wearing an orange jacket with a blue and black helmet is standing, facing the viewer. The figure's helmet is adorned with a blue circular element. The buildings exhibit a dilapidated appearance, with visible signs of wear and rust.
- p9: An image captures a woman wearing sunglasses and a jacket, standing on a boat and smiling. She is wearing a backpack, which is located on her back. The boat is floating on a river, and the water is visible in the background.
- p10: An image features a golden retriever playing in autumn leaves, tongue lolling. Crisp red and orange foliage blankets the ground, with a weathered wooden fence and distant misty mountains framing the scene.

Text-to-Video:

- p1: A close-up shot of a black pan on a stovetop, where two round, golden-brown falafel balls are being fried. The falafel balls are speckled with green herbs and appear crispy on the outside. As the video progresses, a hand enters the frame and flips one of the falafel balls, revealing a similarly cooked side. The hand then removes the fried falafel from the pan, leaving the other ball to continue frying.
- p2: The process of pouring a liquid into a metal cup. The liquid appears to be a dark brown color, possibly a type of coffee or tea. The cup is cylindrical with a flared top and a black handle. The liquid is poured from a clear glass container with a handle. The background is blurred, but it seems to be an indoor setting with a dark surface. The style of the video is a close-up shot, focusing on the action of pouring the liquid into the cup.
- p3: A person is seen using a power tool to grind a piece of metal. The person is wearing black gloves and is holding the power tool with their right hand. The metal is being held in place by a blue vise. As the person grinds the metal, sparks fly out from the point of contact. The background is blurred, but it appears to be a workshop environment.

Image-to-Image:

- p1: redesign this picture into tourism illustration
- p2: Wipe off the bird from the photo.

Video-to-Video:

- p1: Add a hat.

Prompts used in Figure 5

- p1: Finnish forest reindeer foraging lichen in snowbound woods. Antlers crown among pine shadows where snowshoe tracks circle frozen lakes.
- p2: Clouds shimmering over fjord cliffs. Electric-blue wisps ladder midnight skies where satellites streak above inky waters holding mirror galaxies.
- p3: Icelandic glacier caves radiating sapphire light. Frozen corridors wind through ancient ice, shimmering turquoise under headlamps near subterranean waterfalls.
- p4: A biplane soaring above cotton-cumulus clouds. Ragtime echoes from propeller buzz over patchwork landscapes where toy windmills spin on distant hillsides.
- p5: A beautiful girl with flowing chestnut hair and emerald eyes, wearing a sunflower-print sundress. She stands in a lavender field at sunset, holding a vintage book, with golden light highlighting honeybees hovering near purple blooms.
- p6: A large, well-lit bedroom with a bed positioned towards the right side of the room. The bed is adorned with a gold comforter, giving it a luxurious appearance. The room also features a chair on the left side and another chair closer to the center of the room. The overall atmosphere of the bedroom is elegant and inviting.
- p7: A small black and white dog standing on a sandy beach. The dog appears to be looking to the side, possibly observing something or someone in the distance. The dog is wearing a collar, which adds a sense of charm to the scene.
- p8: A large elephant standing in a field with trees and bushes. The elephant is positioned near the center of the scene, surrounded by a variety of trees and bushes. Some of the trees have no leaves, while others have a mix of green and brown leaves. The elephant appears to be grazing or exploring the area, possibly searching for food.
- p9: A ginger cat perched on a moss-covered stone wall, amber eyes wide. Dappled sunlight filters through oak leaves onto its striped fur, with bluebells and ferns crowding the wall's base.

Prompts used in Figure 6

- p1: A video shows a man's face breaking into a warm, genuine smile as he recognizes someone off-camera. The style is candid and heartwarming. The lighting is soft and natural. The overall impression is one of sudden, happy recognition.
- p2: A rabbit hopping through a misty forest floor at dawn, its movements quiet and cautious. The style is atmospheric and mysterious, with the rabbit as a gentle guide through the scene. The lighting is the soft, diffused light of a foggy morning. The overall impression is one of magical, quiet exploration.
- p3: A man's reflection in a puddle on a city street as he walks by. The style is artistic and anonymous. The lighting is the reflected light of the city. The overall impression is one of a fleeting moment in the urban flow.
- p4: A video shows a baby's wide, fascinated eyes as he look up at a colorful mobile spinning above their crib. The style is wondrous and focused, capturing their developing senses. The lighting is soft and colorful, perhaps from the mobile itself. The overall impression is one of a whole new world opening up.

Prompts used in Figure 7

- p1: Add a red flower to the center of the cactus plant.
- p2: Change it into kyoto animation
- p3: Change the color of the clouds to pink
- p4: Change the color of the water to turquoise

Prompts used in Figure 8

- p1: Add a sea.
- p2: Eliminate the man.
- p3: Change the park to beach.
- p4: Add a hat to the woman.